Machine Learning-Based Utilization of Renewable Power Curtailments under Uncertainty by Planning of Hydrogen Systems and Battery Storages

Shams, Mohammad H. ; Niaz, Haider ; Na, Jonggeol ; Anvari-Moghaddam, Amjad; Liu, Jay J.

Published in:
Journal of Energy Storage

DOI (link to publication from Publisher):
https://doi.org/10.1016/j.est.2021.103010

Publication date:
2021

Document Version
Publisher's PDF, also known as Version of record

Journal of Energy Storage 41 (2021) 103010

Contents lists available at ScienceDirect

Journal of Energy Storage

journal homepage: www.elsevier.com/locate/est

Machine learning-based utilization of renewable power curtailments under uncertainty by planning of hydrogen systems and battery storages

Mohammad H. Shams [a], Haider Niaz [b], Jonggeol Na [c], Amjad Anvari-Moghaddam [d], J. Jay Liu [a,b,*]

[a] Institute of Cleaner Production Technology, Pukyong National University, Busan 48547, Republic of Korea
[b] Department of Chemical Engineering, Pukyong National University, Busan 48513, Republic of Korea
[c] Department of Chemical Engineering and Materials Science, Graduate Program in System Health Science and Engineering, Ewha Womans University, Seoul 03760, Republic of Korea
[d] Department of Energy Technology, Aalborg University, 9220 Aalborg, Denmark

ARTICLE INFO

Keywords:
Electrolyzers
Energy storage
Power curtailments
Deep learning
Stochastic programming

ABSTRACT

Increasing wind and solar generation in power grids leads to more renewable power curtailments in some periods of time due to the fast and unpredictable variations of their outputs. The utilization of these sources for energy storage can unlock huge potential benefits. Therefore, aiming at minimizing the curtailments of renewable power from the viewpoint of an independent system operator (ISO), in this paper, we propose deep learning-driven optimal sizing and operation of alkaline water electrolyzers (AWE) and battery energy storage systems (BESS). For this purpose, a set of actual renewable power curtailment data of California ISO was fully investigated, and deep learning forecast methods were employed to determine the prediction error and its probability distribution function (PDF). Using the fitted PDF, a set of scenarios was generated and reduced to some accurate and probable ones. Consequently, a two-stage scenario-based stochastic model was proposed to determine the optimal planning of this system, and a penalty variable was defined in the second stage to maximize the utilization of curtailed renewable energy sources (RESs). The learning results showed that the prediction errors were minimized using the gated recurrent unit (GRU) method. It was also shown that 97% of curtailments were utilized using AWEs with annual costs of $233.55 million, which had 63.5% fewer costs than using BESSs. Furthermore, using AWEs reduced operational expenses by 89.1% compared with using BESSs, owing to their operational benefits.

1. Introduction

The increased share of renewable energy in electric power systems has created new challenges and sometimes leads to oversupply due to the lack of rapid ramp-up/down generating units in power grids. For example, in spring, snowpacks send much water to hydroelectric power plants, leaving less capacity for renewable energy sources (RESs). In such conditions, due to the lack of flexibility of conventional generation systems, energy production from RESs is sometimes curtailed by independent system operators (ISOs) [1] to avoid system contingencies [2]. According to some reports, in 2020, the amount of renewable power curtailments in California ISO (CAISO) has increased by 64% compared with 2019 [3]. Furthermore, on some occasions, the amount of curtailed renewable generation exceeds 10%, such as in China, Italy, and the Electric Reliability Council of Texas (ERCOT) market in the United States [4]. Financial losses as a result of oversupply in the U.S. Pacific Northwest, a hydro-dominated power grid where wind generation is rapidly increasing was examined in [5]. According to the study, increasing wind capacity will increase oversupply, with future electricity prices affecting the amount of the curtailments. Hence, to maximize the utilization of clean RESs, ISOs strive to minimize energy curtailments by implementing energy storage systems, fast, responsive, and flexible units, and demand-side management strategies.

In this regard, to minimize curtailed renewable power by considering environmental issues, in this study, we aimed to introduce an optimal sizing and operation model of alkaline water electrolyzer (AWE) to produce hydrogen and use battery energy storage systems (BESS) to store electricity during oversupply periods. Furthermore, to cope with the volatile nature of wind and solar curtailments, a deep learning

* Corresponding author at: Institute of Cleaner Production Technology, Pukyong National University, Busan 48547, Republic of Korea.
E-mail addresses: m.h.shams1985@gmail.com (M.H. Shams), haider@pukyong.ac.kr (H. Niaz), jgna@ewha.ac.kr (J. Na), aam@et.aau.dk (A. Anvari-Moghaddam), jayliu@pknu.ac.kr (J.J. Liu).

https://doi.org/10.1016/j.est.2021.103010
Received 15 June 2021; Received in revised form 22 July 2021; Accepted 23 July 2021
Available online 4 August 2021

Nomenclature

Indices and acronyms

i	Index of zones $i = 1,2,\ldots,NI$
s	Index of scenarios $s = 1,2,\ldots,S$
t	Index of time $t = 1,2,\ldots,T$
AWE	Alkaline water electrolyzer
$BESS$	Battery energy storage system
CAPEX	Capital expenditure
M	Large constant
MM$	Million-dollar
max/min	Upper/Lower limits
OPEX	O&M expenditure
$O\&M$	Operation and maintenance
RMSE	Root Mean Squared Error [MW]

Variables

$ACC^{i}_{AWE/BESS}$	Annualized capital cost of AWE/BESS in zone i [$]
CAP^{i}_{AWE}	Capacity of AWE in zone i [MW]
CAP^{i}_{BESS}	Capacity of BESS in zone i [MWh]
$C^{i,t}_{p,s}$	Penalty cost of excess power for scenario s and time t [$]
$FOC^{i}_{AWE/BESS}$	Fixed $O\&M$ cost of AWE/BESS in zone i [$/year]
$H^{i,t}_{AWE,s}$	Produced hydrogen of AWE in zone i for scenario s and time t [kg]
$OMC^{i,t}_{AWE/BESS,s}$	Variable $O\&M$ cost of AWE/BESS in zone i for scenario s and time t [$]
$P^{i,t}_{AWE,s}$	Consumed power by AWE in zone i for scenario s and time t [MW]
$P^{i,t}_{ch/dis,s}$	Charge and discharge power of BESS in zone i for scenario s and time t [MW]
$P^{i,t}_{e,s}$	Excess power in zone i for scenario s and time t [MW]
$RC^{i,t}_{BESS,s}$	Annualized replacement cost of BESS in zone i for scenario s and time t [$]
$Sc^{i,t}_{s}$	Scenarios' costs in zone i for scenario s and time t [$]
$u^{i,t}_{ch/dis,s}$	Binary variables show the status of BESS for scenario s and time t

Parameters

$\alpha.$	Coefficients of capacities limitations [%]
$CAP^{i,max}_{AWE}$	Maximum size of AWE [MW]
$CAP^{i,max}_{BESS}$	Maximum size of BESS [MWh]
$CAWE$	Capital cost of AWE per MW [$/MW]
$CBESS$	Capital cost of BESS per MWh [$/MWh]
CRF	Capital recovery factor
η^{i}_{AWE}	Efficiency of AWE in zone i [%]
$\eta^{i}_{ch,dis}$	Efficiency of charge and discharge for BESS in zone i [%]
f_{w,KOH,s,N_2}	Flow of water, potassium hydroxide, steam, and nitrogen [kg/kg of H_2]
ir	Interest rate[%]
LHV_{H_2}	Lower heating value of hydrogen [MWh/kg]
ny	Project lifetime [years]
NC_{BESS}	Number of cycles for BESS charge and discharge
$P^{i,t}_{cs/w,s}$	Curtailed solar and wind power in zone i for scenario s and time t [MW]
π^{FOC}_{BESS}	Fixed $O\&M$ cost of BESS per MW [$/MW-year]
$\pi^{O\&M}_{BESS}$	Variable $O\&M$ cost of BESS per MWh [$/MWh]
π_P	Price of penalty [$/MWh]
π_{w,KOH,s,N_2}	Price of water, potassium hydroxide, steam, and nitrogen per kg of produced hydrogen [$/kg]
π_{dis}, π_{H_2}	Electricity, hydrogen selling prices [$/MWh, $/kg]
R_{BESS}	Range of discharge [%]
ρ_s	Probability of scenarios [%]

Table 1
Comparisons of the studies on the management of power curtailments.

Reference	[6]	[7]	[9]	[11]	[12]	[13]	[14]	[15]	[22]	[23]	[30]	This Study
Minimizing RES curtailments	×	×	✓	✓	✓	✓	✓	✓	✓	×	×	✓
Forecasting RES curtailments	×	×	×	×	×	×	×	×	×	×	×	✓
Short-term operation	✓	×	✓	×	×	✓	✓	✓	×	×	✓	✓
Planning and sizing	✓	✓	×	✓	✓	✓	×	×	✓	✓	✓	✓
Utilizing AWE	✓	✓	✓	✓	✓	✓	×	×	✓	✓	✓	✓
Utilizing BESS	×	×	×	×	✓	×	✓	✓	✓	✓	×	✓
Uncertainty modeling	✓	✓	×	×	×	×	✓	✓	×	✓	×	✓

method was utilized to forecast and generate scenarios for improved operation management through a two-stage stochastic process.

In recent years, several works have focused on optimal sizing [6–8] and the operation scheduling [9,10] of wind-hydrogen systems. In [6], from the perspective of investors, an optimized sizing model for a wind-hydrogen system was developed using a chance-constrained programming approach. The extension of [6] is described in [7], which considers the hydrogen demand and trading modes. Also, a day-ahead dispatching approach for wind-hydrogen systems in power grids with modeling the external characteristics of hydrogen production was proposed in [9]. A net present value objective function for a hybrid offshore wind farm and a hydrogen system was developed in [11], where the interests of investors and effects of power curtailments were evaluated.

In contrast to previous studies, only a few articles have considered the optimal design of solar-hydrogen systems [12,13]. Reference [12] proposed a heuristic approach for the optimal location and size of off-grid solar-hydrogen energy systems based on social, environmental, economic, and technical criteria. Moreover, the optimal planning of energy systems, such as solar photovoltaic power plants, electrolyzers, fuel cells, hydrogen tank storage systems, and chilled/hot water storage systems, was explored in [13]. One common theme among the examined articles is that they aimed at optimizing their problems from an investor's perspective. However, none of them aimed at managing renewable power curtailments in the grid-connected mode of RES power plants.

Furthermore, BESSs have been extensively studied in recent years as possible solutions for alleviating the volatility of RESs [14–21]. In [14], to decrease wind power curtailment during oversupply periods, a two-stage model using BESSs was proposed. The commitment of thermal units and the output of wind turbines are determined in the first stage, while the operation of BESSs is scheduled in the second stage. Also, a risk-based day-ahead operation scheduling model for the unit commitment problem with large wind farms and bulk BESSs was defined in [15]. Moreover, in other studies, BESSs were utilized for peak shaving in

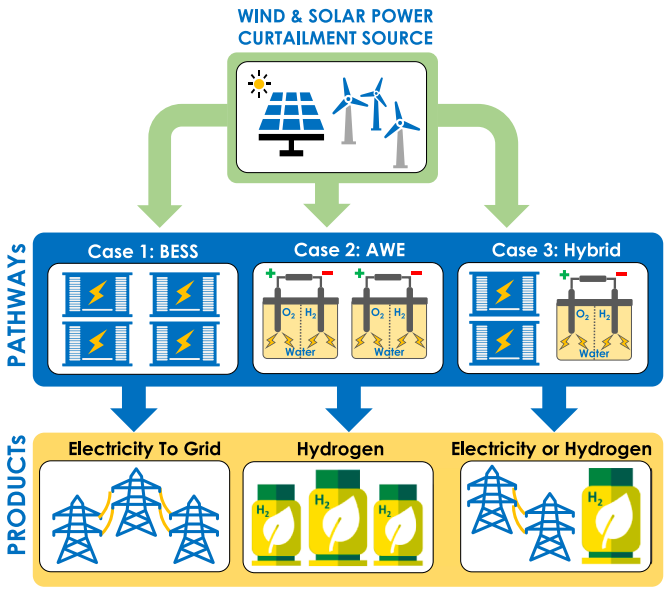

Fig. 1. Schematic of the proposed system.

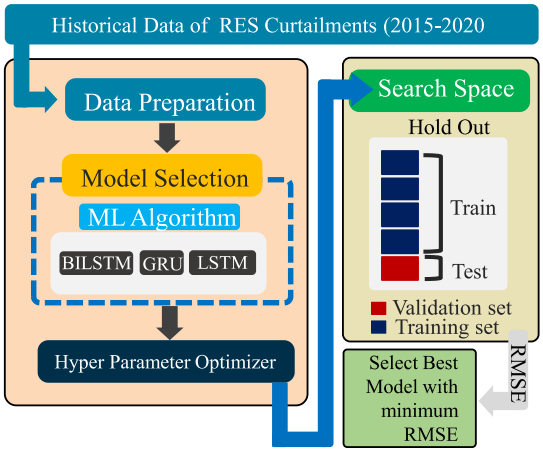

Fig. 2. Flowchart of the RES curtailment prediction.

wind farms [16], and they were found to decrease the effects of forecasting errors [17] and reduce the probable penalties of wind farms by ISOs in electricity markets [18]. Besides, some works [22,23] attempted to utilize both batteries and hydrogen as storage units to support volatile renewable power generation.

The above investigations have mainly focused on the optimal planning of wind/solar-hydrogen systems. The optimal planning of these systems could be unfavorably influenced because of the uncertainties of wind and solar power generation as well as their curtailments. Therefore, forecasting renewable power curtailments and considering the associated uncertainties with enhancing the optimal planning of AWEs and BESSs are crucial issues. Nevertheless, several publications have investigated machine learning or autoregressive models to predict wind and solar generation [24–26] based on historical data. Likewise, some machine learning methods were introduced to generate scenarios for stochastic programming problems [27–29].

To this point, despite the forecasting efforts of wind speed and solar radiations, there have not been any studies on forecasting wind and solar power curtailments. Actually, there are no predictive investigations or straightforward probability distribution functions (PDFs) for the forecasting errors of RES curtailments. Table 1 provides a comprehensive overview of the most relevant existing studies, and it highlights some of their shortcomings and shows our work's merits. So far, there have been very few surveys discussing the optimal size and operation of both AWEs and BESSs for managing oversupply conditions. Also, these studies have mostly ignored the forecasting uncertainties associated with wind and solar curtailments. Below are the contributions of this study, which aimed at filling the knowledge gap discussed above.

In this paper, machine learning-based optimal planning and operation of AWE–BESS systems were proposed to alleviate curtailed RES power using a two-stage stochastic approach. Compared with existing research, the major contributions of the proposed framework are as follows:

- A comprehensive learning-based data analysis was performed based on time-series renewable power curtailment reports obtained from CAISO, and it was utilized as input for training and forecasting procedures. Afterward, a PDF reflecting the errors of the forecasted and actual values was fitted for scenario generation. So far, there have not been any studies on the prediction of renewable power curtailments.
- Compared with the existing deterministic [9,11–13] and chance-constrained models [10,22], in this paper, a two-stage scenario-based planning approach is proposed to cope with the uncertainties associated with wind and solar power curtailments.
- In contrast to the research works in [6,7,9,11,15,23], which only focus on the planning of wind-hydrogen systems, in this study, the comprehensive sizing and operation of AWE–BESS were examined to maximize RES curtailments utilization.
- Unlike most works [7,11], which were performed from an investor's viewpoint, this paper proposes an objective to maximize the utilization of RESs based on the perspective of ISO by incorporating a penalty term in the cost minimization objective.

The proposed scheme in this study is a two-stage scenario-based stochastic operational planning model of AWE and BESS that was developed to maximize the utilization of wind and solar power curtailments, and it was linearized and modeled as a mixed-integer linear programming (MILP) problem, coded in GAMS software, and solved using the CPLEX solver [31]. The machine learning, PDF fitting, and scenario generation approach were implemented in MATLAB, and the generated scenarios were reduced using the SCENRED tool in GAMS software [32].

The rest of this paper is organized as follows. Section 2 represents the preliminaries of the performed work, and the mathematical modeling is described in Section 3. The case studies and results are demonstrated in Section 4, and the conclusions are mentioned in Section 5.

2. Preliminaries

Fig. 1 highlights the proposed schematic and its respective end products. The curtailment option considered in the model comprises both wind and solar curtailment. A total of three pathways were considered in the model, and they were classified as Case 1 (With BESS), Case 2 (With AWE), and Case 3 (With BESS and AWE).

2.1. AWE model

The electrolyzer used in this model is an alkaline water electrolyzer. Among all the available electrolyzer technologies, AWE is a mature and commercially available technology [33]. Many industrial electrolyzers have the capacity to produce 650 m^3 of hydrogen per hour [34]. From an economic point of view, AWE has a longer life span of around 80,000–90,000 h, making it a favorable option for long-term operations [35,36]. In addition to its economic viewpoint, AWE is capable of withstanding low current densities, making it flexible, so it can easily accommodate the dynamic nature of electrolyzers.

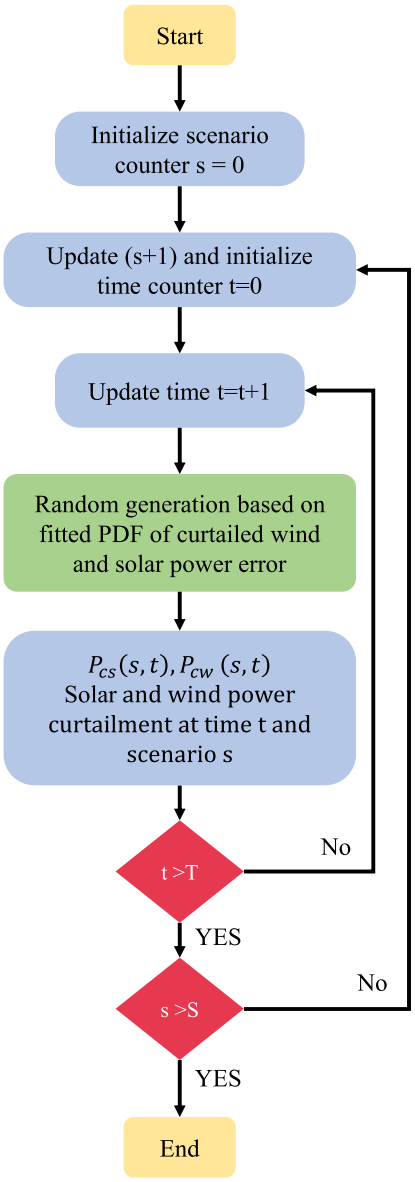

Fig. 3. Flowchart of the scenario generation and reduction approach.

2.2. BESS model

The lithium-ion (Li-Ion) battery technology was used as a BESS in this study, as Li-Ion BESSs offer ample energy storage based on their size and can be frequently charged and discharged during their life spans. In comparison with other technologies, the Li-Ion technology offers the highest system efficiency (86%) and has a very minute degradation rate [37]. Also, apart from its operational benefits, it has the highest manufacturing and technology level, making it the most suitable option in our study.

2.3. Data analysis and deep learning approach

Forecasting RES power curtailments is the main task of ISOs, especially when a system is highly penetrated by wind and solar generation. In this regard, five-year historical data of RES curtailments (2015–2019) was used to train three mature, well-implemented, and widely used machine learning methods: long short-term memory (LSTM) [38], bidirectional LSTM [39], and gated recurrent unit (GRU) [40]. Accordingly, the best method with the least root mean squared error (RMSE) was chosen to forecast wind and solar curtailments one year ahead (i.e., 2020), as shown in Fig. 2. Eq. (1) demonstrates the RMSE, where T denotes the total prediction hours, YP denotes the forecasted values, and YA denotes the actual observed values.

$$RMSE = \sqrt{\frac{1}{T}\sum_{t=1}^{T}(YP - YA)^2} \tag{1}$$

2.3.1. Long short-term memory networks

There is a type of neural network called recurrent neural network (RNN), where the connections between nodes are organized along with a sequential relationship. Thus, temporal dynamic behavior is exhibited. LSTM networks work similarly to RNNs, except that the hidden layer updates are replaced by purpose-built memory cells. Therefore, data with long-range dependencies might be discovered and utilized much better.

The following Eqs. (2)–(6) implement a memory cell of an LSTM network [41]:

$$I_t = \sigma(W_{xI}x_t + W_{hI}h_{t-1} + W_{cI}c_{t-1} + b_I) \tag{2}$$

$$f_t = \sigma\left(W_{xf}x_t + W_{hf}h_{t-1} + W_{cf}c_{t-1} + b_f\right) \tag{3}$$

$$c_t = f_t c_{t-1} + I_t tanh(W_{xc}x_t + W_{hc}h_{t-1} + b_c) \tag{4}$$

$$o_t = \sigma(W_{xo}x_t + W_{ho}h_{t-1} + W_{co}c_t + b_o) \tag{5}$$

$$h_t = o_t \tanh(c_t) \tag{6}$$

where σ, I, f, and o denote sigmoid functions in addition to the input, forget, and output gates, respectively. Also, c and h are cell and hidden vectors, respectively. The weight matrices are W with the same subscripts as those of gates (e.g., W_{cI} is the diagonal matrix of the cell input gate).

2.3.2. Bidirectional long short-term memory networks

Since we had access to both past and future input elements, we could use a bidirectional LSTM network, as proposed in [39]. Thus, the past and future features could be efficiently used for a specific time frame via forward and backward states.

2.3.3. Gated recurrent unit networks

GRU networks were proposed to capture dependencies over time-scales by adapting each recurrent unit [42]. GRU units have gate units that control information flow, just like LSTMs, without separate memory cells. In comparison with those of the LSTM network, GRU consists of the memory cell and new memory cell.

2.4. Uncertainty modeling

To proceed with the uncertainty modeling, the errors of the forecasted and actual observed values were initially fitted to a PDF, which was then utilized to perform scenario generation using the Monte-Carlo approach. Fig. 3 demonstrates the employed algorithm for obtaining the best scenario along with the probabilities. After the scenario generation, the vectors of all the scenarios were reduced to a total of the best and most accurate scenarios using the Fast Backward method in the SCENRED tool in GAMS [31]. Three algorithms are included in SCENRED: The Fast Backward method, Backward/Forward methods, and Backward/Backward methods. Generally, the methods differ in their computation performance (i.e., accuracy and run time). According to the estimated time for running large scenario trees such as our work, the Fast Backward method performs the best. These algorithms employ a distance measure that exploits the difference between the original and reduced probabilities. The probability distance is a compromise between scenario probabilities and their values. As a result, scenarios with a small probability or close to each other will be deleted.

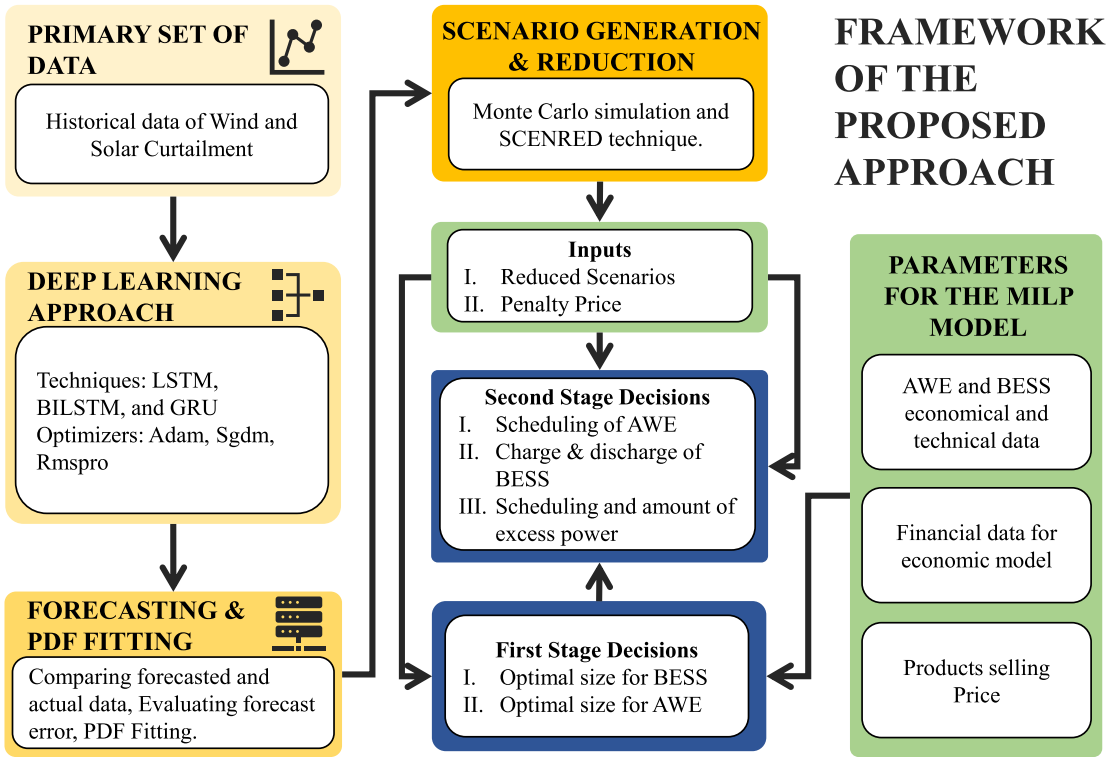

Fig. 4. Framework of the proposed approach.

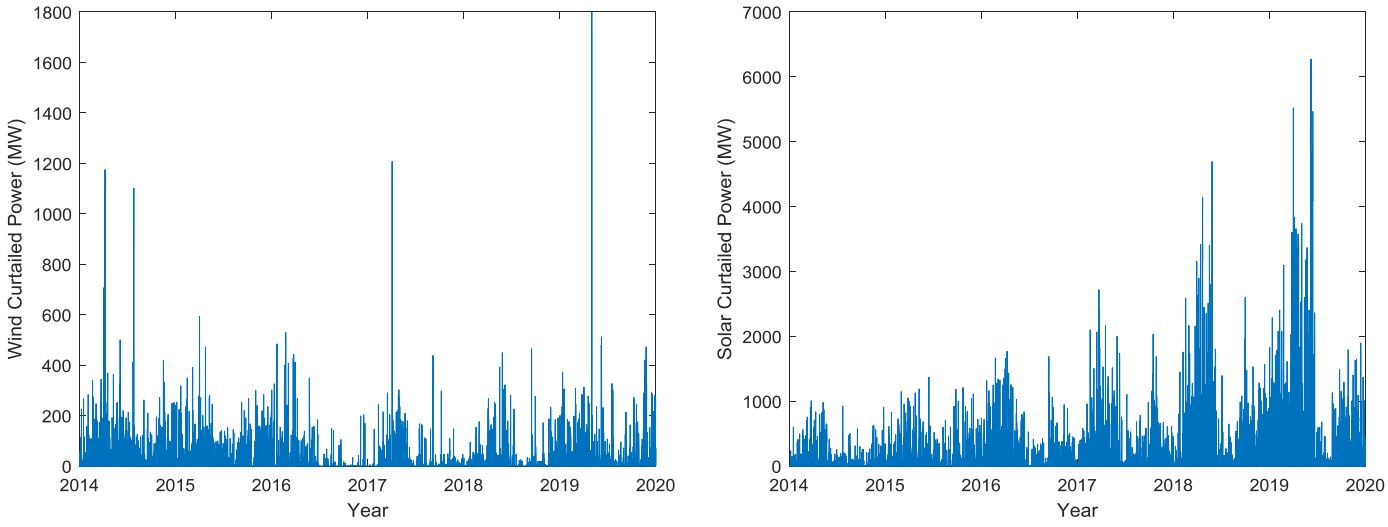

Fig. 5. Wind and solar curtailed power from 2015 to 2020 [3].

Table 2
Summary of the wind and solar curtailed power for 2020.

Reference	Wind	Solar
Total Curtailed Power (MWh)	94,967	1,543,464
Maximum Power Curtailed (MW)	1,799	6,275
No. of Curtailed Hours (hr)	1,584	4,044
Percentage of curtailment hours in a year (%)	18	46
Standard Deviation (MW)	51	521
Mean	10	174

2.5. Assumptions

In our optimization model, the following assumptions were considered:

1) The optimal size of the equipment does not refer to a single unit, and it denotes the total number of units to be installed zone-wide next to wind or solar farms to accommodate RES curtailments.
2) The project life considered is ten years, so the replacement costs of the AWEs were neglected, and no salvage values were considered. For the BESSs, we considered the replacements cost since it depends on the number of charge and discharge cycles.

Table 3
Parameters used in the model.

Parameter	Units	Value	References
$CAWE$	$/MW	298,000	[45]
$CBESS$	$/MWh	380,000	[46]
ir	%	4.50	[47]
ny	Years	10	[47]
π_{BESS}^{FOC}	$/MW-yr	10,000	[37]
$\pi_{BESS}^{O\&M}$	$/MWh	30	[37]
f_{w,KOH,s,N_2}	kg/kg of H_2	10.11, 0.0019, 0.11, 0.00029	[35]
π_{w,KOH,s,N_2}	$/kg	0.012, 2.96, 0.012, 0.33	[35]
LHV_{H_2}	MWh/kg	0.033	[35]
π_P	$/MWh	1000	-
η_{ch}^i, η_{dis}^i	%	95	[37]
η_{AWE}	%	68	[35]
π_{H_2}	$/kg	4.50	[47]
π_{dis}	$/MWh	90	[46]
$\alpha_0, \alpha_1, \alpha_2, \alpha_3, \alpha_4$	%	5,30,30,20,20	[35,37]
R_{BESS}	%	80	[37]
NC_{BESS}	Cycles	35,00	[37]

3) Electricity and hydrogen products are sold at their respective market prices to nearby industries and power grid.
4) The objective function was formulated from an ISO perspective rather than an investor perspective; therefore, the utilization of resources was our main objective, followed by the system operation profits.

3. Proposed two-stage stochastic sizing and operation model

In this part, a two-stage scenario-based sizing and operation framework was modeled as a MILP problem. The objective function was to minimize the yearly expected planning and operation costs of the AWE–BESS system. In the first stage, the optimal sizing of AWE and BESS was determined, while the optimal operation of the system in the generated scenarios was preserved in the second stage. Fig. 4 demonstrates the sequence of the proposed work: data analysis, forecasting, PDF fitting, scenario generation and reduction, and two-stage modeling. As shown in the figure, the decisions related to the optimal sizing of the AWE and BESS units were determined in the first stage, and the decisions pertaining to the scheduling of AWE/BESS and the amount of excess power in the concerned zones were defined in the second stage. Afterward, the objective function and constraints were introduced.

3.1. Objective function

Eq. (7) shows that the objective function is the CAPEX and OPEX minimization model. The annualized capital costs of AWE and BESS were included in CAPEX as (8)–(10), and the operation and penalty costs of excess power were included in OPEX as (11)–(17). In this modeling, the penalty cost of excess power was incorporated in the scenario costs to enforce optimization for maximizing the utilization of curtailed wind and solar power. In better words, the objective function aims at maximizing the utilization of curtailed wind and solar power.

The annualized capital costs of AWE and BESS were calculated in (8) and (9), respectively, using the capital recovery factor equation represented in (10) [43]. Eqs. (11) and (12) define the fixed operation and maintenance costs of AWE and BESS, respectively. The scenarios' cost for Zone i and time t is shown in (13), and it includes the variable operating costs of units (AWE–BESS) and the penalty cost of excess power. The variable O&M cost of the electrolyzer is described in (14) as a function of the produced hydrogen and used water, potassium hydroxide, nitrogen, and steam. The generated hydrogen depends on the consumed power and electrolyzer efficiency, as shown in (15). Eq. (16) defines the O&M cost of BESS using the amount of charged power in each period. Finally, (17) presents the penalty cost of excess power.

$$\underset{CAP_{AWE}^i, CAP_{BESS}^i, P_{AWE,s}^{i,t}, P_{ch/dis,s}^{i,t}, P_{e,s}^{i,t}}{minimize} \sum_{i=1}^{NI} \left\{ \underbrace{ACC_{AWE}^i + ACC_{BESS}^i}_{CAPEX} + \underbrace{FOC_{AWE}^i + FOC_{BESS}^i + \sum_{t=1}^{T} \sum_{s=1}^{S} \rho_s . Sc_s^{i,t}}_{OPEX} \right\} \tag{7}$$

Table 4
Comparative analysis for RMSE based on the used algorithms and optimizers.

Algorithm	Optimizer	RMSE [MW]
LSTM	ADAM	219.83
LSTM	SGDM	346.22
LSTM	RMSPROP	236.60
GRU	ADAM	198.64
GRU	SGDM	321.72
GRU	RMSPROP	209.80
BILSTM	ADAM	287.04
BILSTM	SGDM	359.05
BILSTM	RMSPROP	284.87

*Number of hidden units (NHU) =200, Gate activation function (GAF) = Sigmoid, State action function (SAF) = tanh, Epochs = 250.

$$ACC_{AWE}^i = CAWE . CAP_{AWE}^i . CRF \tag{8}$$

$$ACC_{BESS}^i = CBESS . CAP_{BESS}^i . CRF \tag{9}$$

$$CRF = \frac{ir(1+ir)^{ny}}{(1+ir)^{ny} - 1} \tag{10}$$

$$FOC_{AWE}^i = \alpha_0 . CAP_{AWE}^i . CAWE \tag{11}$$

$$FOC_{BESS}^i = \alpha_2 . CAP_{BESS}^i . \pi_{BESS}^{FOC} \tag{12}$$

$$Sc_s^{i,t} = OMC_{AWE,s}^{i,t} + OMC_{BESS,s}^{i,t} + C_{p,s}^{i,t} \tag{13}$$

$$OMC_{AWE,s}^{i,t} = \left(f_w . \pi_w + f_{KOH} . \pi_{KOH} + f_{N_2} . \pi_{N_2} + f_S . \pi_S\right) . H_{AWE,s}^{i,t} \tag{14}$$

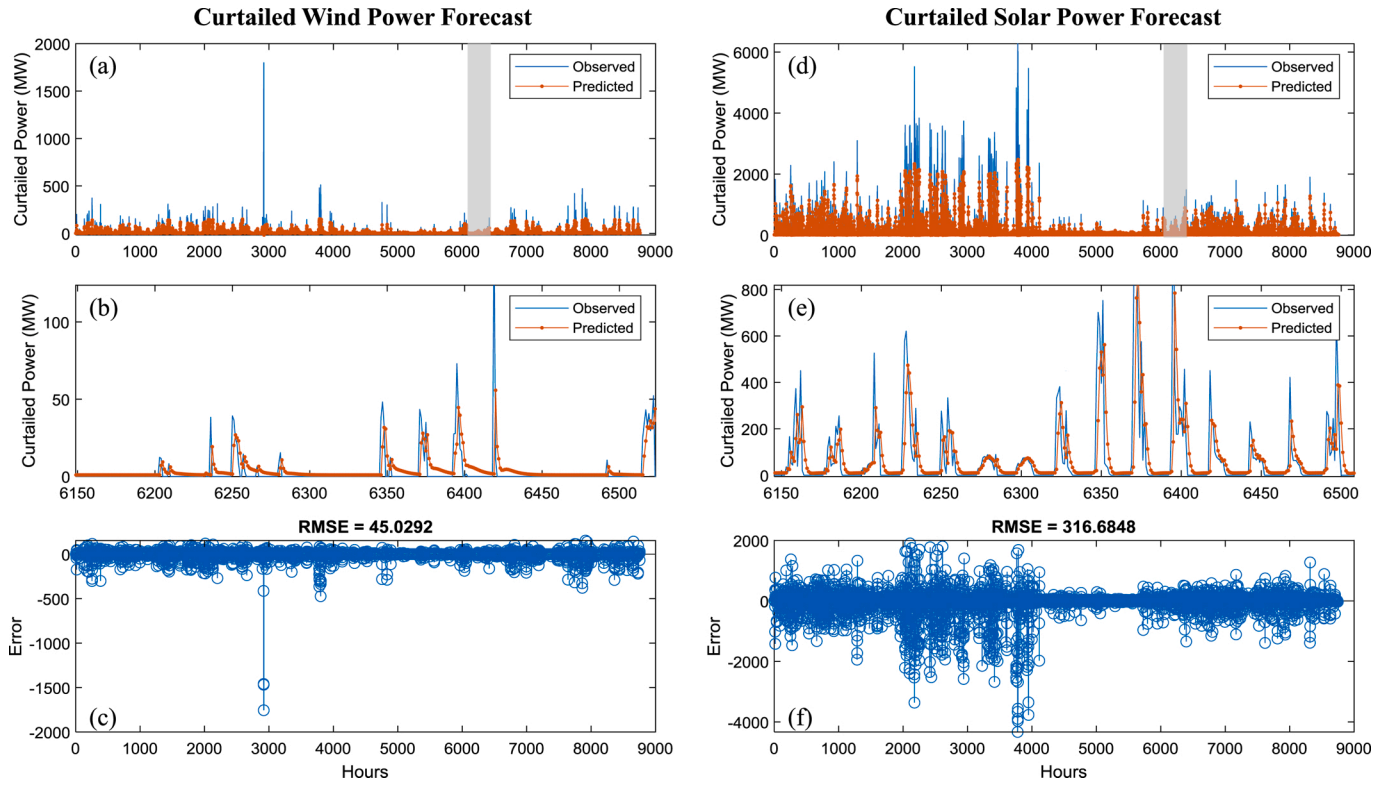

Fig. 6. Wind and solar curtailed power forecasting for the year 2020—(a) curtailed wind forecast, (b) magnified version of the curtailed wind power from 6150 to 6500 h, (c) Error for the wind forecast, (d) curtailed solar forecast, (e) magnified version of the solar curtailed power from 6150 h to 6500 h, and (f) Error for the solar forecast.

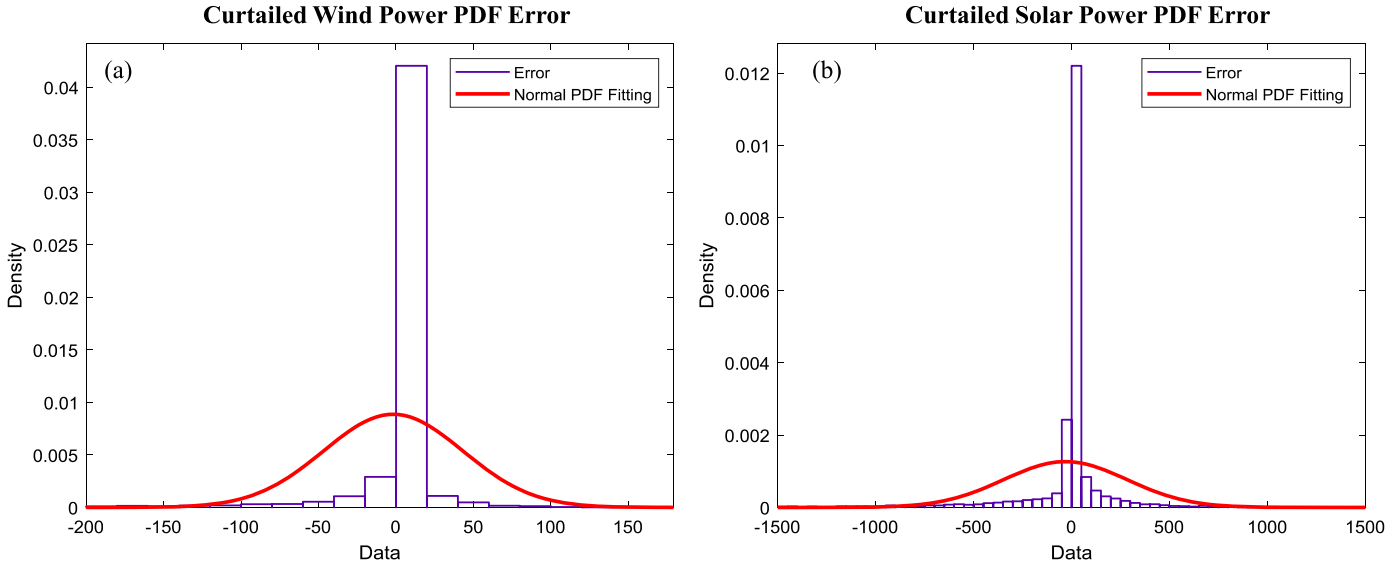

Fig. 7. Error and Normal PDF fitting curve for the (a) wind and (b) solar power curtailments in 2020.

$$H^{i,t}_{AWE,s} = P^{i,t}_{AWE,s}.\eta^{i}_{AWE}/LHV_{H_2} \quad (15)$$

$$OMC^{i,t}_{BESS,s} = \pi^{O\&M}_{BESS}.P^{i,t}_{ch,s} \quad (16)$$

$$C^{i,t}_{p,s} = P^{i,t}_{e,s}.\pi_P \quad (17)$$

3.2. Constraints

The constraints were considered in three parts: 1) first-stage constraints associated with the planning and sizing of the AWE and BESS units in the concerned zones, 2) second-stage constraints regarding the O&M costs in the scenarios, and 3) linking constraints between the first and second stages.

3.2.1. First-stage problem

The maximum and minimum acceptable capacities of BESSs and AWEs for each zone in the planning stage were considered in (18) and (19), respectively.

$$CAP^{i,min}_{BESS} \leq CAP^{i}_{BESS} \leq CAP^{i,max}_{BESS} \quad (18)$$

Table 5
AOC, CAPEX, OPEX, penalty cost, product, profits, system size, and utilization of the curtailed power.

Reference	Units	Case 1	Case 2	Case 3
Objective (AOC)	MM$	640.00	233.55	270.00
CAPEX	MM$	240.00	130.00	94.10
OPEX	MM$	38.50	4.16	3.93
Penalty cost	MM$	352	48.50	136
Electricity Product	MWh	1,042,032	-	-
Hydrogen Product	ton/year	-	32,304	30,600
Profit	MM$	(184.71)	11.18	39.66
AWE size	MW	-	3,462	2,500
BESS size	MWh	5000	-	-
Utilization	%	79	97	92

MM$: Million dollars

Table 6
Comparison of the obtained results with deterministic models.

Reference	Units	Case 1	Case 1 (DET*)	Case 2	Case 2 (DET)	Case 3	Case 3 (DET)
Objective (AOC)	MM$	640	646	233	230	270	272
Utilization	%	79	79	97	97	92	91.6

* DET is the deterministic model

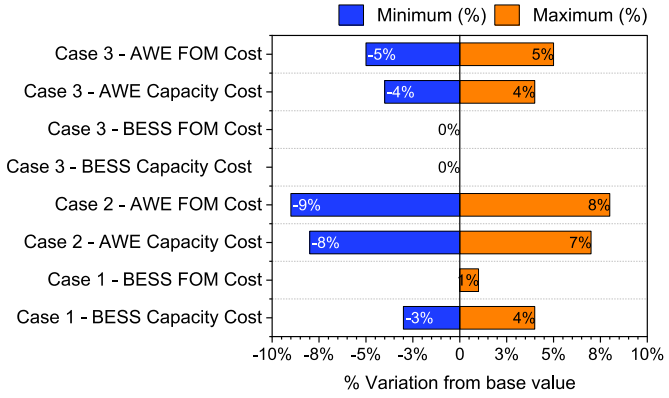

Fig. 8. One-point sensitivity analysis for Cases 1, 2, and 3.

$$CAP^{i,min}_{AWE} \le CAP^{i}_{AWE} \le CAP^{i,max}_{AWE} \tag{19}$$

3.2.2. Second-stage problem

The summation of the consumed power in AWE, charged power in BESS, and excess power should be equal to the amount of curtailed RES power in each zone, time, and scenario, as shown in (20). Moreover, (21) shows the balance of the state of charge in BESSs in each period.

$$P^{i,t}_{e,s} + P^{i,t}_{ch,s} + P^{i,t}_{AWE,s} = P^{i,t}_{cs,s} + P^{i,t}_{cw,s} \tag{20}$$

$$SOC^{i,t}_{s} = SOC^{i,t-1}_{s} + \eta^{i}_{ch}.P^{i,t}_{ch,s} - P^{i,t}_{dis,s} \Big/ \eta^{i}_{dis} \tag{21}$$

3.2.3. Linking the first and second-stage problems

As described in (22) and (23), respectively, the allowable amount of charge and discharge in each BESS is a portion of the BESS capacity. Constraint (24) guarantees that the state of charge in BESSs is within a certain range. Constraints (25)–(27) restrict the BESSs from being simultaneously charged and discharged. The consumed power of the electrolyzer is limited within its capacity, as shown in (28).

$$0 \le P^{i,t}_{ch,s} \le \alpha_1.CAP^{i}_{BESS} \tag{22}$$

$$0 \le P^{i,t}_{dis,s} \le \alpha_2.CAP^{i}_{BESS} \tag{23}$$

$$\alpha_3.CAP^{i}_{BESS} \le SOC^{i,t}_{s} \le CAP^{i}_{BESS} \tag{24}$$

$$P^{i,t}_{ch,s} \le u^{i,t}_{ch,s}.M \tag{25}$$

$$P^{i,t}_{dis,s} \le u^{i,t}_{dis,s}.M \tag{26}$$

$$u^{i,t}_{ch,s} + u^{i,t}_{ch,s} \le 1 \tag{27}$$

$$\alpha_4.CAP^{i}_{AWE} \le P^{i,t}_{AWE,s} \le CAP^{i}_{AWE} \tag{28}$$

3.2.4. Modeling the BESS replacement cost

In order to consider the annualized replacement cost of the BESS in the modeling, the below equation is defined [44]. Based on this model, the replacement cost primarily depends on the range and number of charges and discharges, as shown in (29).To consider the replacement cost, (29) should be added to the scenario costs as in (13).

$$RC^{i,t}_{BESS,s} = \frac{\eta^{i}_{ch}.P^{i,t}_{ch,s}.CBESS}{R_{BESS}.NC_{BESS}} \tag{29}$$

4. Case studies and numerical results

4.1. Data and scenarios

The 2015–2020 wind and solar curtailment data used for the analysis and sizing was taken from California ISO [3]. The curtailment data was recorded for different hours and at different minute intervals, and it was only sorted for one-hour intervals to keep consistency. A year-round curtailment data distribution for the wind and solar profiles can be seen in Fig. 5 from 2015 to 2020. It can be observed from Fig. 5 that the wind curtailment was less than the solar curtailment due to the prevalence of solar installation in California. In this system, the average load is 25,827 MW, the average power exchange is 6805 MW, and the output power of solar farms, wind turbines, nuclear power plants, large hydro units, thermal power plants, and other renewables plants (i.e., biomass or geothermal) are 2814 MW, 1685 MW, 2020 MW, 2439 MW, 8312 MW, 6250 MW, respectively.

Table 2 summarizes the total curtailed power, highlighting the maximum curtailed power at a particular hour and the number of times power was curtailed per year. Solar power had the highest curtailment due to its higher installation capacity. A total of 1.5 million MWh of power was curtailed, accounting for 46% of the curtailment hours a year. As for wind power, curtailment occurred for 1584 h a year, representing 18% of the total hours a year. This curtailed power can unlock potential benefits for profits, so it was extensively studied, as shown in the following sections.

The values of the considered parameters in this study are shown in Table 3. These parameters include the capital and operation costs, technical and financial parameters, and efficiencies of AWEs and BESSs.

Sorted data sets of five years from 2015 to 2019 with 43,800 points were input as training values to the deep learning algorithm. The LSTM, GRU, and BILSTM methods were employed in MATLAB to analyze the RMSE score for the year 2020, along with a combination of different optimizers, as shown in Table 4. The parameters used for training are mentioned in the footnotes of Table 4.

It can be observed that BILSTM has poor performance and that it resulted in high RMSE. Besides, the BILSTM predictions had a huge deviation from the zero value for the times with no solar radiation, which is not practically possible. Thus, BILSTM was neglected and was not considered for further analysis. The LSTM and GRU algorithms performed better than BILSTM, with predictions near zero when no solar radiation was available. Among all, the GRU algorithm and ADAM [48] optimizer resulted in the lowest RMSE score for both the wind and solar

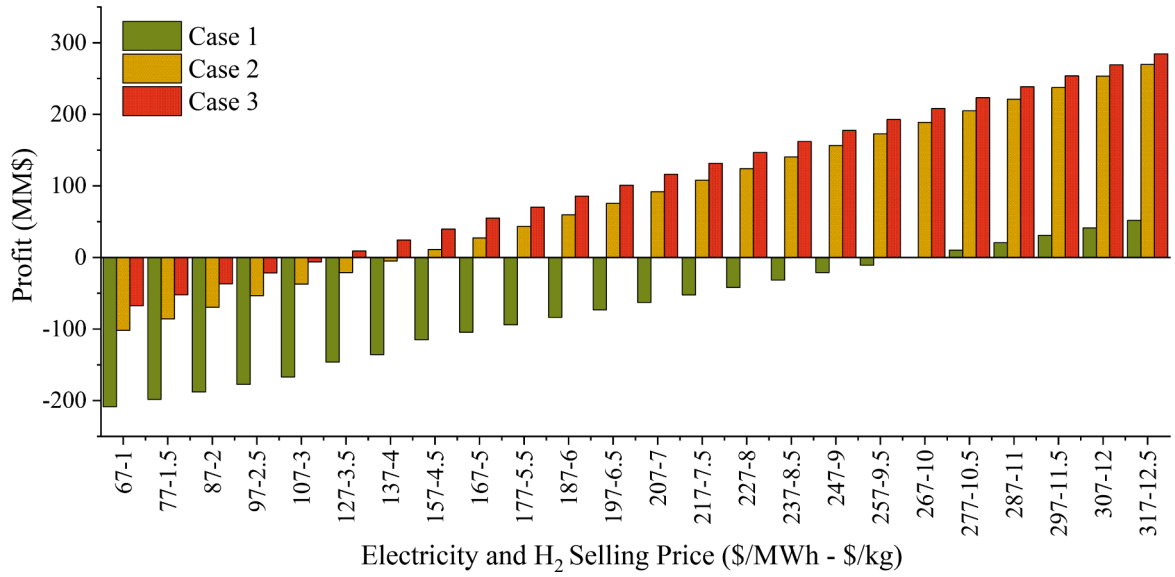

Fig. 9. Effect of the electricity and hydrogen prices on profit—Case 1 shows the effect of the electricity selling price on profit when varied (67–317 $/MWh); Cases 2 and 3 show the effect of the hydrogen selling price on profit when varied (1–12.5 $/MWh).

curtailed data. Thus, GRU and ADAM were chosen to individually predict the wind and solar curtailments for the year 2020, as shown in Fig. 6. The forecasted wind and solar data, as well as observed values in the respective year, i.e., 2020, are shown in Fig. 6 (a) and (d). To have a better look at the predicted and observed values, a magnified time slot was demonstrated, as shown in Fig. 6 (b) and (e). Finally, Fig. 6 (c) and (f) show the RMSE score at individual hours, with plus and minus values depicting the difference between the predicted and observed data. Using the error data obtained from the predicted values, a normal PDF was fitted to be used as input in the generation scenario. The error PDF distribution can be seen in Fig. 7. The mean and standard deviations for the wind power curtailment were -1.77 and 44.99, whereas they were -31 and 315.12 for the solar power curtailment, respectively. These values were used in the Monte-Carlo scenario-generation approach, as shown in Fig. 3. A set of 100 scenarios were generated and reduced to the best and most accurate five scenarios.

4.2. Results

As shown in Fig. 1, the proposed model was applied to three cases to alleviate wind and solar power curtailments by 1) only BESSs in Case 1, 2) only AWEs in Case 2, and 3) both AWEs and BESSs in Case 3. It should be noted that the maximum size was kept similar (i.e., 5000 MW) for both Case 1 and Case 2. For Case 3, the maximum allowable size was equally distributed between the AWE (2500 MW) and BESS (2500 MW). Cases 1, 2, and 3 were evaluated for their total expected annual operating cost (AOC). As explained in the formulation section, the system costs, i.e., BESS and AWE equipment costs, were annualized only to evaluate the yearly operating costs and annual profits for each case scenario. Furthermore, for each case scenario, the fraction of the curtailed power utilization was also evaluated. A summary of the results for Cases 1, 2, and 3 can be seen in Table 5 for the first scenario.

4.2.1. Case 1: with Battery Energy Storage System (BESS)

Owing to the high technology costs of BESSs compared with AWEs, BESS resulted in high CAPEX and high OPEX. Keeping in mind the objective function, i.e., maximization of utilization, Case 1 hit its upper bound of 5000 MW. To achieve the maximum possible curtailment utilization, the case results in the maximum possible size for BESS satisfied the given objective. As a result, Case 1 had no profit ($184.71 million of loss) and had more operational costs. Annually, the system only consumed a total of 79% of curtailed power. As the system could not completely utilize the curtailed power given the size constraint, the utilized curtailed power was penalized. The penalty cost was 46.6% higher than with CAPEX for Case 1, which is a major contributor to the high annual costs of Case 1. Therefore, the optimal size for Case 1 was the same as the upper bound considered in the model, i.e., 5000 MW. It should be noted that considering the replacement cost of the BESS in the formulation increased the AOC from $640 million to $819 million and had no effect on other variables such as capital costs, utilization, and BESS size, as shown in Table 5; Because the objective function was based on maximizing the utilization of the RES curtailment and not based on cost minimization.

4.2.2. Case 2: with Alkaline Water Electrolyzer (AWE)

Case 2, in contrast to Case 1, had 63.5% less annual costs, i.e., $233.55 million, as shown in Table 5. Owing to the operational benefits of AWE, the operational cost of Case 2 was $4.16 million, which is 89.1% less than that of Case 1. As hydrogen has a greater benefit as a storage medium, the difference in the penalty costs between Cases 1 and 2 can be seen in Table 5. Compared with Case 1, Case 2 had 86.2% fewer penalty costs due to its high utilization of curtailed power (96%). Annually, Case 2 could utilize 1,567,500 MWh of power for converting it to hydrogen. This amount of power can result in the annual production of 35,604 tons of hydrogen and an annual operating profit of $11.18 million. The optimal size for Case 2 to accommodate curtailed power is 3,404 MW. Among all the cases, Case 2 showed to have the highest utilization rate and second-highest profit.

4.2.3. Case 3: hybrid case (BESS + AWE)

Case 3 considers the hybrid case, where both BESS and AWE are utilized. For Case 3, the upper bounds for the maximum power for BESS and AWE were reduced to half compared with the maximum bounds used in Case 1 and Case 2, respectively, i.e., 2500 MWh for the BESS state of charge and 2500 MW for the AWE capacity. To satisfy the objective of maximum utilization, Case 3, similar to Case 1, hit its upper bound, as shown in Table 5. At an AWE size of 2500 MW, Case 3 can utilize 92% of the curtailed power and produce 33,730 tons of hydrogen annually. Also, Case 3 showed to have the highest profits among all cases, corresponding to $39.6 million. High profits are due to less CAPEX as the AWE size was reduced by 26.5%, which equally lays off the expenses from AOC. It should be noted that in Case 3, the replacement cost

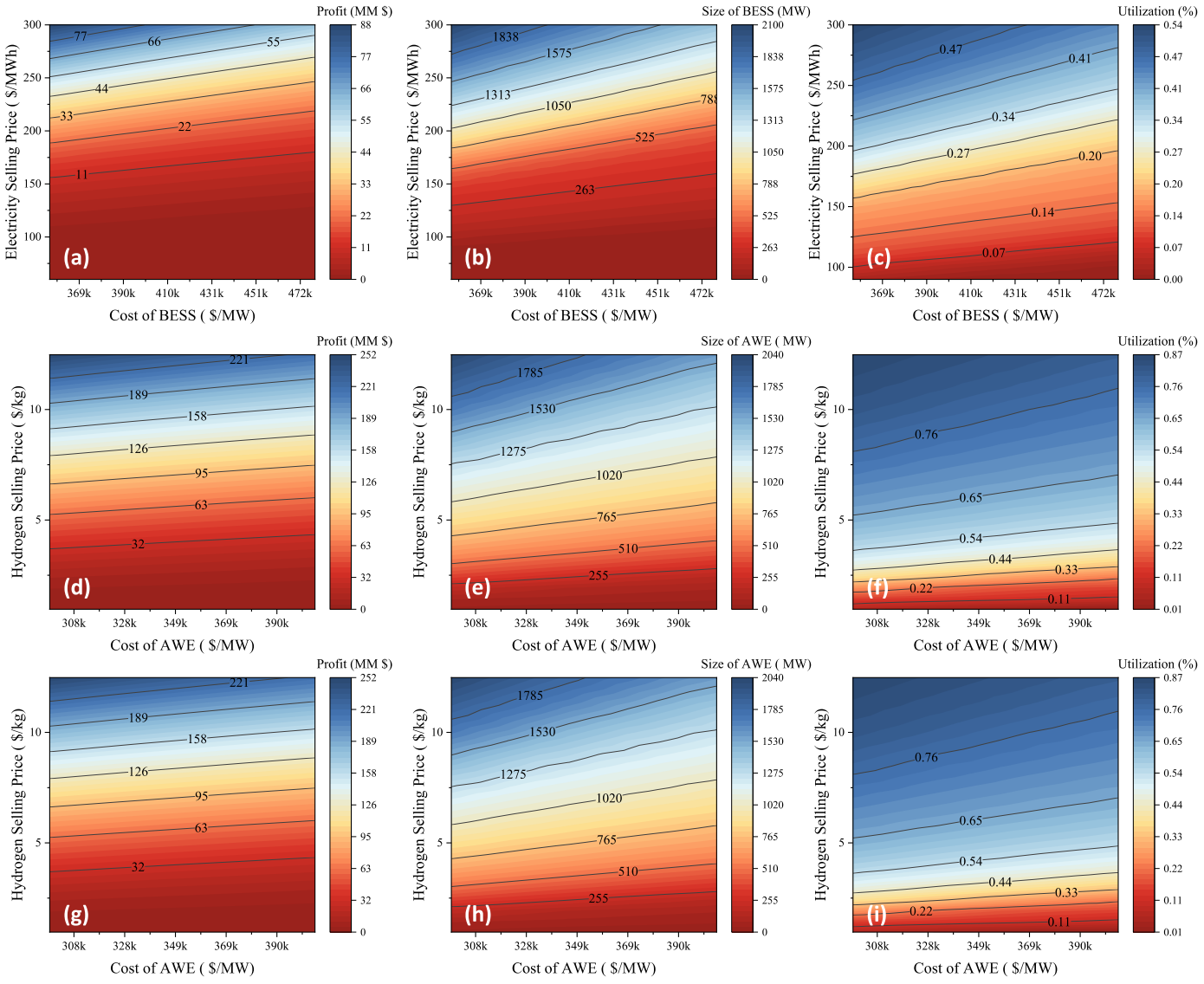

Fig. 10. Effects of the product selling price and system cost on profit, system sizing, and utilization via profit maximization—(a), (b), and (c): Case 1 profit, BESS size, and utilization; (d), (e), and (f): Case 2 profit, AWE size, and utilization; and (g), (h), and (i): Case 3 profit, AWE size, and utilization.

of BESS did not have any effects because the BESSs were not employed due to their high capital and operation costs.

4.3. Model validation

This section has validated the proposed two-stage stochastic model by comparing it with the deterministic model. For the deterministic model, the predicted wind and solar curtailments were used as the input for the model. As shown in Table 6, the proposed two-stage stochastic method had almost similar AOC and utilization with respect to the deterministic methods. Results validated the proposed model and showed the effectiveness of the approach in the context of stochastic planning and operation.

4.4. Discussion and sensitivity analysis

Cases 1–3 were subjected to one-point sensitivity analysis to observe the expected variations in the AOC due to market fluctuations and technology price. For these fixed operational and maintenance costs (FOM) for BESS and AWE, the technology cost (BESS and AWE) was considered as a sensitive parameter. Fig. 8 shows the results of the one-point sensitivity analysis.

For Case 1, the BESS capacity had the highest impact on AOC. With a 10% increase in the BESS capacity cost, there was a 4.0% increase in the AOC. However, with a 10% decrease in FOM, no change was observed. Similarly, for Case 2, the AWE technology cost had the second-highest impact, followed by the FOM of AWE. The impact of FOM on AOC can be justified due to the higher utilization rate for Case 2. Lastly, for Case 3, as AWE was selected as an optimal option for the utilization of curtailed power, the FOM of BESS and the BESS capacity cost had no impact on the cost. Furthermore, similar to Case 2, the FOM of AWE had the highest impact, followed by the AWE capacity cost.

4.5. Effects of the product price, system cost, and penalty

4.5.1. Effect of the electricity and hydrogen price on the profit/cost minimization

The electricity and hydrogen prices do not impact the utilization of curtailed power, but their selling price highly affects the profit for each case scenario. For Case 1, electricity is the product, whereas for Cases 2 and 3, hydrogen is the product. The base electricity price used in the model to calculate the system's profit is 90 $/MWh, whereas the selling price of hydrogen was considered as 4.5 $/kg in the model. These prices

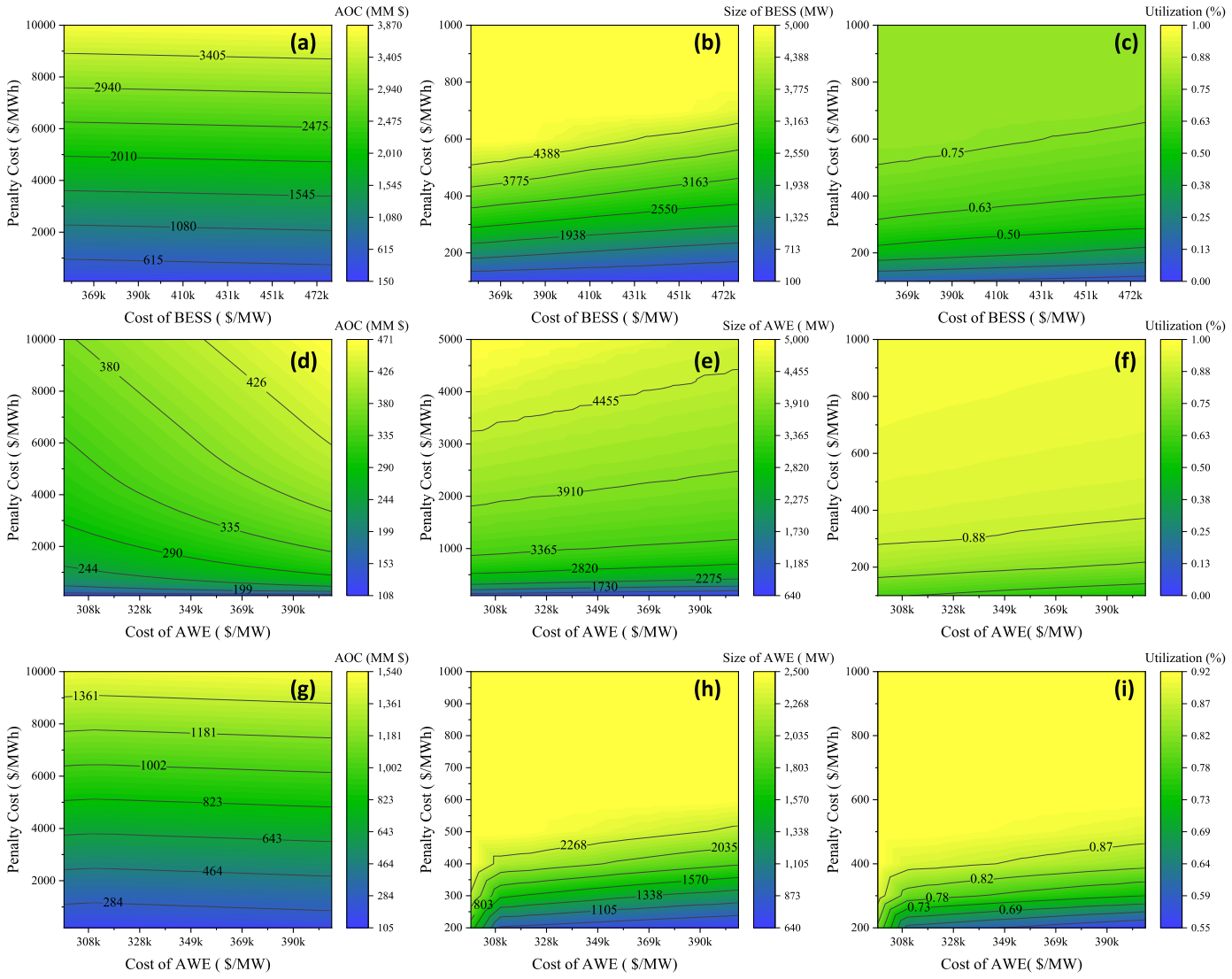

Fig. 11. Effects of the penalty price and system cost on the AOC, system sizing, and utilization via the AOC objective function—(a), (b), and (c): AOC, BESS size, and utilization of Case 1; (d), (e), and (f): AOC, AWE size, and utilization of Case 2; and (g), (h), and (i): AOC, AWE size, and utilization of Case 3.

are varied respectively from the lower bounds of 67 $/MWh and 1 $/kg to the maximum bounds of 317 $/MWh and 12.5 $/kg for electricity and hydrogen. The resulting profits can be seen in Fig. 9 for Cases 1, 2, and 3, respectively. It must be noted that the profit was evaluated from the results obtained via the cost minimization objective function. An analysis via the profit maximization objective function with a varying product selling price and a penalty price can be seen in the next section.

The minimum selling price at which Case 1 started to generate profit is 268 $/MWh. Below this price, the profit is negative, i.e., the operating expenses are more than the operational savings. Similar to Case 2, the minimum selling price was calculated to be 4.15, whereas, for Case 3, it was calculated to be 3.2 $/kg. The price for Case 3 decreased by 29.6% compared with Case 2, generating more economical benefits. However, Case 2 showed to have a better utilization rate in comparison with Case 3.

4.5.2. Effects of the product selling price and system cost (Profit Maximization)

After the one-point sensitivity analysis, the effects of the product selling price and system size on profit, system size (BESS or AWE), and utilization of curtailed power were evaluated using the profit maximization objective function. The profit maximization objective is the same as AOC. Also, it is constrained without considering the penalty cost and considers the revenue from selling electricity and hydrogen. Thus, the electricity selling price for Case 1 varied from a minimum of 60 $/MWh to a maximum of 300 $/MWh. Similar to Cases 2 and 3, the hydrogen selling price varied from a minimum of 1 $/kg to a maximum of 12.5 $/kg. Likewise, the system costs for BESS and AWE varied from the minimum values of 355k $/MW and 298k $/MW to the maximum values of 478k $/MW and 405k $/MW, respectively. The profit maximization results can be seen in Fig. 10.

From Fig. 10 (a), it can clearly be seen that Case 1 resulted in a maximum profit of $88.2 million and that it failed to generate any profit with an electricity selling price below 90 $/MWh. In contrast, Case 2 showed a profit increase of 85.7%, as shown in Fig. 10 (d). Case 3 had similar results to those of Case 2, as the profit maximization was driven toward a smaller system size, which eventually ended up to be the same for both cases, as seen in Fig. 10 (g). Since this particular case is for profit maximization, the utilization of curtailed power was not the primary goal. This overview of the profits can be a good reference source from an investor's perspective. The results for the sizing and curtailment utilization of Case 1 can be seen in Fig. 10 (b) and (c). With profit maximization, Case 1 had an optimal size of 2100 MW with the lowest equipment cost and highest electricity selling price and could only accommodate 54% of the curtailed power. As shown in Fig. 10 (e), (f),

and (h), (i), Case 2 had a 2.8% lower system size for the lowest system cost and maximum hydrogen selling price. With a system size of 2040 MW, Cases 2 and 3 resulted in a 60.7% increase in the utilization of curtailed power compared with Case 1, i.e., 86.8%. The results showed that from a profit perspective, Cases 2 and 3 have the best to offer.

4.5.3. Effects of the penalty price and system Cost (AOC Minimization)

The effects of the penalty price and system size on the AOC, system size (BESS or AWE), and utilization of curtailed power were evaluated using the AOC objective function. For this, the penalty prices for Cases 1, 2, and 3 varied from a minimum of 100 $/MWh to a maximum of 10,000 $/MWh. Likewise, the system costs for BESS and AWE varied in a similar manner, as mentioned in the previous section. The results of the AOC objective function can be seen in Fig. 11.

As shown in Fig. 11, the objective function aimed at minimizing the AOC with a subjected penalty price, thus deriving the optimization toward maximum utilization to avoid penalties. The optimizer opted for a maximum system size for all the cases. It must be noted that since the penalty price increased from a minimum of 100 to 10,000 $/MWh, the AOC increased with the increased penalty price, as seen in Fig. 11 (a), (d), and (g), respectively. Therefore, although the optimal size reached its maximum value, the penalty cost was at a higher value, making the AOC much higher than the one at the lower price. As shown in Fig. 11 (b), the maximum system size was realized at a penalty price of ~600–800 $/MW. Above 800 and up to 10,000 $/MW, the system size of BESS was stagnant as the upper bound was already reached. So, for ease of observation, the penalty price scale was lowered to 1000 $/MW from its original maximum value of 10,000 $/MW. A similar trend regarding the system size saturation can be seen in Fig. 11 (e) and (h). However, as shown in Fig. 11 (e), it must be noted that Case 2 reached its saturation level near 900–1000 $/MWh, whereas Case 3 reached its saturation level at ~500–600 $/MWh, as shown in Fig. 11 (h). This is due to the lower upper limit of the hybrid case compared with Cases 1 and 2, with an upper limit of 5000 MW. Lastly, the utilization rate for Cases 1 and 2 was highest with 100% curtailment utilization, whereas for Case 3, the maximum achieved curtailment utilization was 91.7%. All the cases show higher utilization in comparison with the scenarios discussed for profit maximization. The curtailment utilization results for Cases 1, 2, and 3 can be seen in Fig. 11 (c), (f), (i), respectively.

5. Conclusions

Due to the increasing numbers of wind and solar farms, renewable energy curtailment increases with each year. However, energy storage options, such as hydrogen and battery storage systems, can minimize energy curtailments if RESs can be appropriately employed. Therefore, in this paper, we developed a novel deep learning-based planning model for maximizing the utilization of curtailed wind and solar power using the storage capacity of hydrogen and battery systems. RES uncertainty was modeled using a scenario-based two-stage stochastic method. Also, year-ahead scenarios for wind and solar curtailments were generated using a fitted error PDF via a deep learning forecasting approach.

The deep learning results showed that the GRU algorithm could forecast wind and solar power curtailments with a minimal forecast error. Also, the generated scenarios with the obtained forecast errors, when used to run the stochastic model, showed that the hybrid case (i.e., AWE and BESS) is the most profit-generating case. Despite being a hybrid case, the optimal size only resulted in incorporating AWE for the whole zones. Furthermore, the AWE sizing selection highly depended on the penalty price as well as the curtailment amount in the scenarios. However, in some periods with high curtailed power, the optimum AWE size did not increase and was penalized as excess power as a result of the performed cost-benefit assessment. Furthermore, it was revealed that by developing AWE units to produce hydrogen, 97% of the curtailed renewable power could be utilized while taking into consideration the worst curtailment scenarios. The payback period for this investment can be less than five years, with a hydrogen selling price of 6 $/kg and without considering any revenues from monetizing carbon-free sources. Furthermore, the effects of the product selling price and penalties were investigated using AOC and profit objective optimizations.

All in all, this study provides a tangible solution that can be utilized by ISOs for overcoming energy curtailment issues through the effective prediction of renewable energy curtailments, two-stage stochastic equipment sizing, and daily operation for each case. However, the main limitation for implementing this study is the lack of RES curtailment data for other locations. Furthermore, this survey can be extended by utilizing other sources to mitigate the oversupply, such as flexible power plants, demand-side management, and electric and hydrogen vehicles.

Author Contributions

M.H.S. and H.N.: Conceptualization, Methodology, Software, Formal Analysis, Data Curation, Visualization, Writing-Original Draft and Writing – Review and Editing. J.J.L.: Writing – Review and Editing, Supervision and Funding Acquisition., J.N.: Writing – Review and Editing, and A.A.M. Writing – Review and Editing.

Declaration of Competing Interest

The authors declare no competing interests.

Data for reference

The data set and code used in this study will be made available on request to the corresponding author.

Acknowledgments

This research was supported by Basic Science Research Program through the National Research Foundation of Korea (NRF), funded by the MIST (2019R1A2C2084709, 2021R1A4A3025742).

References

[1] A Olson, RA Jones, E Hart, J. Hargreaves, Renewable curtailment as a power system flexibility resource, Electr. J. 27 (2014) 49–61, https://doi.org/10.1016/j.tej.2014.10.005.
[2] C Li, H Shi, Y Cao, J Wang, Y Kuang, Y Tan, et al., Comprehensive review of renewable energy curtailment and avoidance: a specific example in China, Renew. Sustain. Energy Rev. 41 (2015) 1067–1079, https://doi.org/10.1016/j.rser.2014.09.009.
[3] California ISO – managing oversupply n.d. http://www.caiso.com/informed/Pages/ManagingOversupply.aspx (accessed June 8, 2021).
[4] L Bird, D Lew, M Milligan, EM Carlini, A Estanqueiro, D Flynn, et al., Wind and solar energy curtailment: a review of international experience, Renew. Sustain. Energy Rev. 65 (2016) 577–586, https://doi.org/10.1016/j.rser.2016.06.082.
[5] Y Su, JD Kern, GW. Characklis, The impact of wind power growth and hydrological uncertainty on financial losses from oversupply events in hydropower-dominated systems, Appl. Energy 194 (2017) 172–183, https://doi.org/10.1016/j.apenergy.2017.02.067.
[6] Y Jiang, Z Deng, S. You, Size optimization and economic analysis of a coupled wind-hydrogen system with curtailment decisions, Int. J. Hydrogen Energy 44 (2019) 19658–19666, https://doi.org/10.1016/j.ijhydene.2019.06.035.
[7] Z Deng, Y. Jiang, Optimal sizing of wind-hydrogen system considering hydrogen demand and trading modes, Int. J. Hydrogen Energy 45 (2020) 11527–11537, https://doi.org/10.1016/j.ijhydene.2020.02.089.
[8] MH Shams, M Kia, A Heidari, D. Zhang, Optimal design of photovoltaic solar systems considering shading effect and hourly radiation using a modified PSO algorithm, Simulation 95 (2019), https://doi.org/10.1177/0037549719831362.
[9] F Wei, Q Sui, X Li, X Lin, Z. Li, Optimal dispatching of power grid integrating wind-hydrogen systems, Int. J. Electr. Power Energy Syst. 125 (2021), 106489, https://doi.org/10.1016/j.ijepes.2020.106489.
[10] MH Shams, M Shahabi, M MansourLakouraj, M Shafie-khah, JPS. Catalão, Adjustable robust optimization approach for two-stage operation of energy hub-based microgrids, Energy 222 (2021), https://doi.org/10.1016/j.energy.2021.119894.
[11] S McDonagh, S Ahmed, C Desmond, JD. Murphy, Hydrogen from offshore wind: Investor perspective on the profitability of a hybrid system including for

curtailment, Appl. Energy 265 (2020), 114732, https://doi.org/10.1016/j.apenergy.2020.114732.
[12] G Zhang, Y Shi, A Maleki, M. A. Rosen, Optimal location and size of a grid-independent solar/hydrogen system for rural areas using an efficient heuristic approach, Renew. Energy 156 (2020) 1203–1214, https://doi.org/10.1016/j.renene.2020.04.010.
[13] J Liu, Z Xu, J Wu, K Liu, X. Guan, Optimal planning of distributed hydrogen-based multi-energy systems, Appl. Energy 281 (2021), 116107, https://doi.org/10.1016/j.apenergy.2020.116107.
[14] X Dui, G Zhu, L. Yao, Two-stage optimization of battery energy storage capacity to decrease wind power curtailment in grid-connected wind farms, IEEE Trans. Power Syst. 33 (2018) 3296–3305, https://doi.org/10.1109/TPWRS.2017.2779134.
[15] A Nikoobakht, J Aghaei, M Shafie-Khah, JPS. Catalao, Minimizing wind power curtailment using a continuous-time risk-based model of generating units and bulk energy storage, IEEE Trans. Smart Grid 11 (2020) 4833–4846, https://doi.org/10.1109/TSG.2020.3004488.
[16] P Zhao, J Wang, Y. Dai, Capacity allocation of a hybrid energy storage system for power system peak shaving at high wind power penetration level, Renew. Energy 75 (2015) 541–549, https://doi.org/10.1016/j.renene.2014.10.040.
[17] F Luo, K Meng, ZY Dong, Y Zheng, Y Chen, KP. Wong, Coordinated operational planning for wind farm with battery energy storage system, IEEE Trans. Sustain. Energy 6 (2015) 253–262, https://doi.org/10.1109/TSTE.2014.2367550.
[18] X Xu, W Hu, D Cao, Q Huang, W Liu, C Chen, et al., Economic feasibility of a wind-battery system in the electricity market with the fluctuation penalty, J. Clean. Prod. 271 (2020), 122513, https://doi.org/10.1016/j.jclepro.2020.122513.
[19] MZ Oskouei, B Mohammadi-Ivatloo, M Abapour, M Shafiee, A. Anvari-Moghaddam, Privacy-preserving mechanism for collaborative operation of high-renewable power systems and industrial energy hubs, Appl. Energy 283 (2021), 116338, https://doi.org/10.1016/j.apenergy.2020.116338.
[20] NS Rayit, JI Chowdhury, N. Balta-Ozkan, Techno-economic optimisation of battery storage for grid-level energy services using curtailed energy from wind, J. Energy Storage 39 (2021), 102641, https://doi.org/10.1016/j.est.2021.102641.
[21] FR Segundo Sevilla, D Parra, N Wyrsch, MK Patel, F Kienzle, P Korba, Techno-economic analysis of battery storage and curtailment in a distribution grid with high PV penetration, J. Energy Storage 17 (2018) 73–83, https://doi.org/10.1016/j.est.2018.02.001.
[22] S Kharel, B. Shabani, Hydrogen as a long-term large-scale energy storage solution to support renewables, Energies 11 (2018), https://doi.org/10.3390/en11102825.
[23] G Yang, Y Jiang, S. You, Planning and operation of a hydrogen supply chain network based on the off-grid wind-hydrogen coupling system, Int. J. Hydrogen Energy 45 (2020) 20721–20739, https://doi.org/10.1016/j.ijhydene.2020.05.207.
[24] M Afrasiabi, M Mohammadi, M Rastegar, S. Afrasiabi, Advanced deep learning approach for probabilistic wind speed forecasting, IEEE Trans. Ind. Inform. 17 (2021) 720–727, https://doi.org/10.1109/TII.2020.3004436.
[25] H Wang, Z Lei, X Zhang, B Zhou, J. Peng, A review of deep learning for renewable energy forecasting, Energy Convers. Manag. 198 (2019), 111799, https://doi.org/10.1016/j.enconman.2019.111799.
[26] M Khodayar, O Kaynak, ME. Khodayar, Rough deep neural architecture for short-term wind speed forecasting, IEEE Trans. Ind. Inform. 13 (2017) 2770–2779, https://doi.org/10.1109/TII.2017.2730846.
[27] Chen Y, Wang Y, Kirschen D, Zhang B. Model-free renewable scenario generation using generative adversarial networks. ArXiv 2017;33:3265–75. https://doi.org/10.1109/pesgm40551.2019.8974096.
[28] SI Vagropoulos, EG Kardakos, CK Simoglou, AG Bakirtzis, JPS. Catalão, ANN-based scenario generation methodology for stochastic variables of electric power systems, Electr. Power Syst. Res. 134 (2016) 9–18, https://doi.org/10.1016/j.epsr.2015.12.020.
[29] M Cui, D Ke, Y Sun, D Gan, J Zhang, BM. Hodge, Wind power ramp event forecasting using a stochastic scenario generation method, IEEE Trans. Sustain. Energy 6 (2015) 422–433, https://doi.org/10.1109/TSTE.2014.2386870.
[30] G He, DS Mallapragada, A Bose, CF Heuberger, E. Gencer, Hydrogen supply chain planning with flexible transmission and storage scheduling, IEEE Trans. Sustain. Energy 3029 (2021) 1–11, https://doi.org/10.1109/TSTE.2021.3064015.
[31] GAMS – cutting edge modeling n.d. https://www.gams.com/ (accessed March 24, 2021).
[32] SCENRED n.d. https://www.gams.com/33/docs/T_SCENRED.html (accessed March 30, 2021).
[33] P Haug, B Kreitz, M Koj, T. Turek, Process modelling of an alkaline water electrolyzer, Int. J. Hydrogen Energy 42 (2017) 15689–15707, https://doi.org/10.1016/j.ijhydene.2017.05.031.
[34] V Subramani, A Basile, TN Veziroğlu, Compendium of Hydrogen Energy, Elsevier, 2015, https://doi.org/10.1016/C2014-0-02671-8.
[35] W Kuckshinrichs, T Ketelaer, JC. Koj, Economic analysis of improved alkaline water electrolysis, Front. Energy Res. 5 (2017) 1, https://doi.org/10.3389/fenrg.2017.00001.
[36] H Niaz, MM Lakouraj, J. Liu, Techno-economic feasibility evaluation of a standalone solar-powered alkaline water electrolyzer considering the influence of battery energy storage system: a Korean case study, Korean J. Chem. Eng. 38 (2021) 1–17, https://doi.org/10.1007/s11814-021-0819-z.
[37] K Mongird, V Fotedar, V Viswanathan, V Koritarov, P Balducci, B Hadjerioua, et al., Energy Storage Technology and Cost Characterization Report, 2019.
[38] S Hochreiter, J. Schmidhuber, Long short-term memory, Neural Comput. 9 (1997) 1735–1780, https://doi.org/10.1162/neco.1997.9.8.1735.
[39] A Graves, J. Schmidhuber, Framewise phoneme classification with bidirectional LSTM and other neural network architectures, Neural Netw. 18 (2005) 602–610, https://doi.org/10.1016/j.neunet.2005.06.042. Pergamon.
[40] K Cho, B Van Merriënboer, C Gulcehre, D Bahdanau, F Bougares, H Schwenk, et al., Learning phrase representations using RNN encoder-decoder for statistical machine translation, in: EMNLP 2014 – 2014 Conf. Empir. Methods Nat. Lang. Process. Proc. Conf., Association for Computational Linguistics (ACL), 2014, pp. 1724–1734, https://doi.org/10.3115/v1/d14-1179.
[41] Huang Z, Xu W, Yu K. Bidirectional LSTM-CRF models for sequence tagging 2015.
[42] J Chen, H Jing, Y Chang, Q. Liu, Gated recurrent unit based recurrent neural network for remaining useful life prediction of nonlinear deterioration process, Reliab. Eng. Syst. Saf. 185 (2019) 372–382, https://doi.org/10.1016/j.ress.2019.01.006.
[43] S Kwon, W Won, J. Kim, A superstructure model of an isolated power supply system using renewable energy: development and application to Jeju Island, Korea, Renew. Energy 97 (2016) 177–188, https://doi.org/10.1016/j.renene.2016.05.074.
[44] EI Vrettos, SA. Papathanassiou, Operating policy and optimal sizing of a high penetration RES-BESS system for small isolated grids, IEEE Trans. Energy Convers. 26 (2011) 744–756, https://doi.org/10.1109/TEC.2011.2129571.
[45] Study on development of water electrolysis in the EU Final Report E4tech Sàrl with Element Energy Ltd for the Fuel Cells and Hydrogen Joint Undertaking. 2014.
[46] Vimmerstedt LJ, Akar S, Augustine CR, Beiter PC, Cole WJ, Feldman DJ, et al. 2019 annual technology baseline. Golden, CO (United States): 2019. https://doi.org/10.2172/1566062.
[47] H Niaz, B Brigljevic, YB Park, HC Woo, JJ. Liu, Comprehensive feasibility assessment of combined heat, hydrogen, and power production via hydrothermal liquefaction of Saccharina japonica, ACS Sustain. Chem. Eng. 8 (2020) 8305–8317, https://doi.org/10.1021/acssuschemeng.0c01951.
[48] DP Kingma, JL. Ba, Adam: a method for stochastic optimization, in: 3rd Int. Conf. Learn. Represent. ICLR 2015 - Conf. Track Proc., International Conference on Learning Representations, ICLR, 2015.